Journal of Physiology (1993), **469**, *pp.* 213–243
With 12 figures
Printed in Great Britain

CORRELATION OF PRIMATE RED NUCLEUS DISCHARGE WITH MUSCLE ACTIVITY DURING FREE-FORM ARM MOVEMENTS

BY L. E. MILLER, P. L. E. VAN KAN*, T. SINKJÆR†, T. ANDERSEN†, G. D. HARRIS‡ AND J. C. HOUK

From the Department of Physiology, Northwestern University Medical School, 303 East Chicago Avenue, Chicago, IL 60611, USA

(*Received 21 August 1992*)

SUMMARY

1. We recorded from 239 neurons located in the magnocellular division of the red nucleus of four alert macaque monkeys. At the same time, we recorded electromyographic (EMG) signals from as many as twenty electrodes chronically implanted on muscles of the shoulder, arm, forearm and hand. We recorded EMG signals for periods ranging from several months to a year.

2. The monkeys were trained to perform three free-form food retrieval tasks, each of which activated all of the recorded muscles and most of the neurons. The 'prehension' task required simply that the monkey grasp a piece of food from a fixed point in space. The 'barrier' task required the monkey to reach around a small barrier to obtain the food, and the 'Kluver' task required that food be removed from small holes. During the prehension task, we found approximately equal numbers of neurons that were strongly active while the hand was being moved toward the target (70% of units), and while the food was being grasped (60%). Relatively few units were active as the hand was returned to the mouth (15%).

3. Data files of 1–2 min duration were collected while the monkey performed a single behavioural task. Whenever possible, we recorded files for all three tasks from each neuron. For each file we calculated long time-span analog cross-correlations ($\pm 1{\cdot}28$ s) between instantaneous neuronal firing rate and each of the full-wave rectified, low-pass filtered EMG signals. We used the peak correlation and the time of the peak as two summary measures of the functional relation between modulation of neuronal activity and EMG.

4. The magnitude of the strongest correlations was between 0·4 and 0·5 (normalized to a perfect correlation of $\pm 1{\cdot}0$). Distal muscles were the most frequently correlated, and extensors were more frequently correlated than flexors. For all monkeys, the lags for well correlated muscles were distributed broadly about

Current addresses:
* Division of Neurobiology, Barrow Neurological Institute, 350 W. Thomas Road, Phoenix, AZ 85013, USA.
† Department of Medical Informatics and Image Analysis, Aalborg University, Fr. Bajersvej 7D, DK-9220 Aalborg, Denmark.
‡ Department of Surgery, Northwestern University Medical School and the Northwestern Memorial Hospital, 448 E. Ontario, Chicago, IL 60611, USA.

MS 1718

a uni-modal value near 0 ms. Eighty five per cent of the correlations larger than or equal to 0·25 had peaks between −150 and 200 ms.

5. The activity of each neuron was represented in a muscle co-ordinate system by an n-dimensional 'functional linkage vector', each element of which was the peak correlation with one of n muscles. The vector for any given neuron points in a particular direction in muscle space, depending on the similarity between the activity of the neuron and the activity of each muscle. Sequential files recorded from a given neuron during a single behaviour yielded very similar linkage vectors, whereas the vectors for different neurons pointed in quite different directions in muscle space. The variation in linkage vectors for any given cell tested repeatedly during different behaviours was intermediate between that of the same cell–same task condition and the different cell–same task condition. Therefore, the correlation between the activity of the magnocellular red nucleus (RNm) neurons and limb muscles is not completely invariant for different tasks, but it varies less than for different RNm neurons.

6. A distinct advantage of the cross-correlation method is its suitability for use with EMG signals, which are otherwise difficult to analyse quantitatively, particularly during free-form movements. By studying EMG, we were able to make meaningful comparisons between quite wide ranging types of behaviour. Because there was essentially no subjective judgement required on the part of the experimenter, the method was both objective and efficient. The resulting functional linkage vectors provide information that is important for understanding how sets of neurons and muscles are used in a variety of natural behaviours.

INTRODUCTION

The co-ordination of limb movements in reaching and grasping is provided by neural commands that are sent to the spinal cord from the magnocellular red nucleus (RNm) and the motor cortex (Kuypers, 1981). These signals, which are transmitted in the rubrospinal tract (RST) and the corticospinal tract (CST), represent the outputs from a complex premotor network comprising interconnections between the cerebellar nuclei, motor cortex, red nucleus and brainstem reticular formation (Allen & Tsukahara, 1974). This limb premotor network has multiple recurrent pathways, and it has been suggested that positive feedback through the recurrent circuits may serve as an important driving force in the generation of the descending commands that control limb movement (Houk, 1989).

There is considerable evidence that movement commands are encoded in a distributed fashion across a large population of these neurons (Houk, Keifer & Barto, 1993). Ultimately, the commands are transmitted to the spinal cord via a large number of fibres which converge on spinal interneurons and motoneurons. The pathway from motor cortex to limb movement is highly convergent. As a result, the system is redundant; a given movement may be produced by more than one pattern of muscle activity, and by extension, a great variety of patterns of neuronal activity. It is likely that particular combinations of neurons are 'chosen' by the nervous system to produce these movements for reasons that we do not yet understand. We have begun to use the analog cross-correlation equation as a means of studying the

co-ordination between patterns of neuronal and EMG activity that occur during free-form movement.

Georgopoulos and his colleagues (Georgopoulos, Kalaska, Caminiti & Massey, 1982) have made some progress in understanding the distributed motor command present in the motor cortex for simple pointing movements. Their studies indicate that single-cell discharge is broadly tuned to the direction of limb movement in space. Although large populations of neurons fire during most limb movements, particular cells are activated maximally for movements in particular directions. For movements other than in its preferred direction, a neuron fires less strongly. A simple weighted vector sum of the population activity proved capable of predicting the direction of limb motion (Georgopoulos, Kalaska, Crutcher, Caminiti & Massey, 1984). A similar coding scheme has been reported for the cerebellum (Fortier, Kalaska & Smith, 1989), and the parietal cortex (Kalaska, Cohen, Prud'homme & Hyde, 1990). Thus, it seems feasible that the entire limb premotor network might utilize a similar population code in generating distributed motor commands to control limb movement.

While it is likely that limb movements are controlled by distributed motor commands, the neural representations used in coding spatial and temporal features of these commands are not clear. Spatial features could be represented in world co-ordinates, which might facilitate the use of vision in planning movements (Paillard, 1991). At the other extreme, commands could be coded in muscle co-ordinates, which would facilitate their implementation (Berthier, Singh, Barto & Houk, 1993). Mussa-Ivaldi (1988) used a mathematical proof to demonstrate that present data on population activity can be interpreted either way. However, if coding schemes requiring different co-ordinate systems existed in different areas of the CNS, some mechanism for translating between them would be required. If the premotor network were to operate in world co-ordinates, there would have to be a transformation somewhere along the rubrospinal and corticospinal pathways to produce movement commands coded in muscle co-ordinates. This would not be required if the premotor network were to operate in muscle space. Instead, mechanisms might be required for converting from retinal to motor co-ordinates at a stage prior to the premotor network.

While considerable work has been done to relate rubrospinal (RST) and corticospinal tract (CST) activity to motion in world co-ordinates, less work has been devoted to exploring relations in muscle co-ordinates. Other efforts to compare modulation of neuronal activity and EMG have tended to rely on comparison of the time of onsets, offsets, peaks, or inflexion points in the two signals. The inherent noise of the two signals often causes these subjective judgements to be rather difficult to make reliably. The signal-to-noise ratio can be improved by averaging repeated trials, but this approach is impossible for free-form movements. Spike-triggered averaging is a well-established method for revealing fluctuations in EMG which are time-locked to individual spike occurrences. This method has proved useful for analysing synaptic connections between premotor neurons and individual muscles. It does not, however, provide information about the functional relation between modulation in the rate of action potentials and EMG activity.

In this paper, we describe the use of the cross-correlation function to study the

strength and reliability of the functional relations between modulations in the activity of single RNm neurons, and the related modulations of limb electromyographic activity. We have found that the discharge of a given RNm neuron expressed in a muscle co-ordinate system remains time-invariant for a given task, and to a lesser extent, task invariant, as compared to the variety of discharge patterns found for different neurons. Preliminary descriptions of these studies have been published in summary form (Miller, Harris & Houk, 1989; Sinkjær, Andersen, Miller & Houk, 1990; Miller, Sinkjær, Andersen, Laporte & Houk, 1992).

METHODS

Subjects

We recorded EMG and neuronal data from four monkeys, two *Maccaca mulata* (AL and BR) and two *Maccaca fascicularis* (GU and MQ). GU and MQ were instrumental in establishing the methods for recording from chronically implanted EMG electrodes over long periods of time. Relatively few signals were recorded successfully from these monkeys, and consequently most of the data reported here, unless otherwise noted, were collected from AL and BR.

Behavioural tasks

The monkeys were trained to perform three different free-form food retrieval tasks. All were self-paced, the only reward being a small piece of food which the animal was required to retrieve. Each monkey was trained to perform all of the tasks, and would switch readily between them.

In the 'prehension' task, the monkey was required to reach toward and grasp a small piece of food (raisin or piece of apple) held by the experimenter. Care was taken that the food was held consistently at shoulder height and nearly arm's length in front of the monkey. The food was given without resistance when the monkey grasped it. Between trials, the monkey returned its hand to the lap, and several seconds elapsed before another piece of food was presented.

In the 'barrier' task, the monkey was required to grasp a piece of food from a small ledge shielded by a clear plastic barrier. The barrier was held in front of the monkey in a variety of locations and orientations during collection of the data file. This forced the monkey to use a wide range of strategies to obtain the food, and thereby varied the temporal patterns of muscle activity.

The third free-form task involved removal of food from a Kluver board. Ten holes ranged in size from 12 to 25 mm, and of either 5 or 10 mm depth. Food was replaced in the wells as the monkey performed the task, resulting in a continuous sequence of arm and hand movements between Kluver board and mouth, interspersed with repeated scooping movements of the digits.

Surgical procedures

After training, the monkeys were subjected to a surgical procedure to implant the recording devices. All surgery was performed under aseptic conditions with either barbiturate (sodium pentobarbitone, 25–30 mg/kg I.V.) or halothane/nitrous oxide (1·0–1·5% halothane + 20–50% nitrous oxide) anaesthesia. The monkeys received Combiotic (Pfizer) antibiotic prophylactically on the morning of the surgery, and for 3–5 days following surgery. Intramuscular injections of Buprenex (Reckitt and Colman; 0·02 mg/kg I.M.), a long-lasting analgesic, were also given for several days, until the monkey's behaviour returned to normal, and it appeared to be suffering little or no pain.

During the surgery, we implanted a recording chamber in a coronal plane approximately 6 mm anterior of Horsley–Clarke zero, 1 cm from the mid-line, and angled 15 deg off vertical. We also implanted an EMG electrode assembly, consisting of 10, 15 or 20 bi-polar electrodes connected to a micro-miniature connector (ITT Cannon). For monkeys MQ and GU, the connector was anchored to the skull, along with the recording chamber. The electrodes consisted simply of the bared ends of the Teflon-coated, stainless-steel miniature cable sutured within the belly of the muscle (Loeb & Gans, 1986). Recurring problems with infection at the wound margin where the bundle of wires entered the acrylic cap prompted us to adopt different methods for monkeys AL and BR.

For these monkeys, we fabricated an electrode assembly consisting of a connector and fifteen or twenty Silastic 'patch' electrodes (Loeb & Gans, 1986). Spacing between the recording surfaces ranged from 5·0 to 1·5 mm for the largest to smallest muscles respectively. The soldered connections

were insulated with Epoxy resin, then covered with a layer of Silastic medical adhesive. The connector itself was cemented to the centre of an oval piece of surgical Dacron felt approximately 3×5 cm in size. Figure 1 shows one such assembly with twenty electrodes prior to implantation.

During surgery, incisions were made above each of the muscles to be implanted. Another incision was made on the monkey's back, parallel to and several centimetres lateral of the spinal cord, and immediately caudal of the scapula. Subcutaneous tunnels were opened from the incision in the back

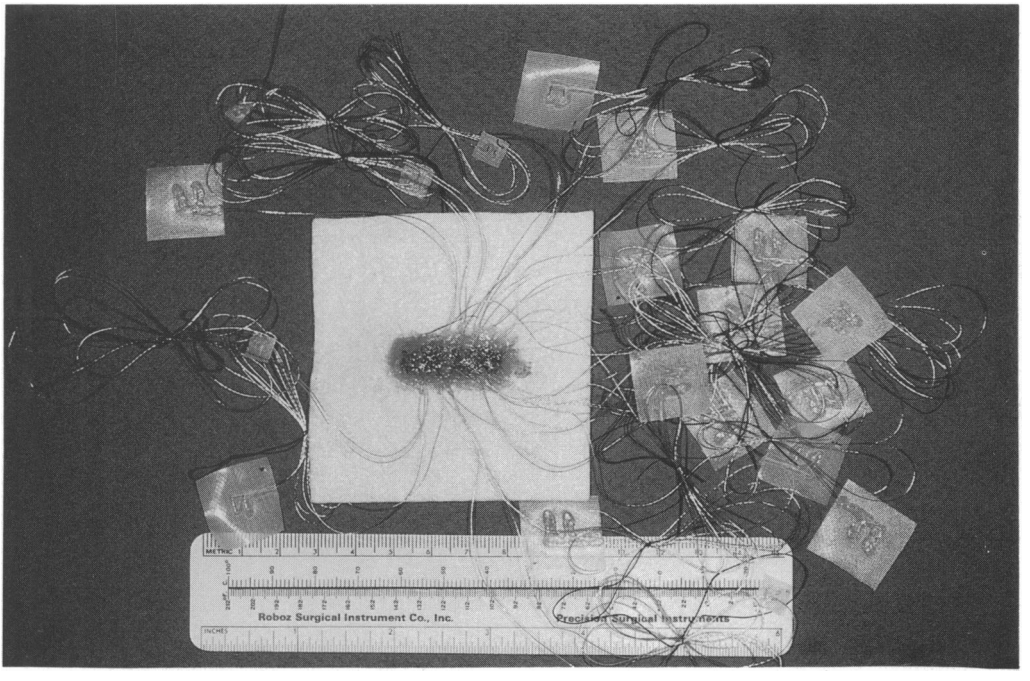

Fig. 1. The EMG electrode assembly before implantation in monkey BR. This view shows the underside of the Dacron patch; the connector leads and soldered connections have been insulated with Epoxy resin, and subsequently covered with Silastic medial adhesive. The Dacron was trimmed before implantation beneath the skin of the monkey's back. The 20 patch electrodes were tunnelled subcutaneously to muscles of the shoulder, limb and hand. Note the 5 mm wide patch immediately to the left of the connector, which was implanted on an intrinsic hand muscle.

to each of the muscles, and the electrodes were passed to the appropriate sites, and sutured onto the surface of each muscle. Among the four monkeys, we implanted the following muscles: serratus anterior, latissimus dorsi, anterior and posterior deltoid, pectoralis, triceps, biceps, brachialis, brachioradialis, pronator teres, flexor carpi ulnaris and radialis, extensor carpi ulnaris and radialis, flexor digitorum superficialis and profundus, extensor digitorum communis, extensor pollicis longus, flexor pollicis brevis, adductor pollicis, 2nd lumbrical, and 1st dorsal interosseous. In the first two monkeys (MQ and GU), electrodes were implanted in the long head of triceps, in monkey AL we implanted in the lateral head, and in monkey BR, in the medial head. Electrodes implanted on the 2nd lumbrical muscle were actually wrapped around the muscle, because of its very small size. The connector was positioned between the skin and muscles, and sutures were passed through the Dacron felt and into the skin. The Dacron provided a good medium for ingrowth of skin, to anchor the connector and improve would healing. A fibreglass cast was placed over the arm and trunk to prevent the monkey from gaining access to the wounds. The cast and dressings were changed at least twice during recovery.

The back-mounted Dacron mesh–connector assembly greatly reduced problems with infection.

Infection localized to the connector site occurred occasionally in both monkeys, but did not threaten the health of the animal, nor the integrity of the electrodes. Good signals were still being recorded from eleven of the fifteen electrodes in monkey AL four months after implantation at the end of the experiments. Eighteen of the twenty electrodes implanted in monkey BR continued to produce good signals a full year after implantation.

Neuronal recordings and histological localization

Neuronal recordings were made with Epoxylite-coated tungsten microelectrodes having an impedance between 0·25 and 1 MΩ. During initial recording sessions for each monkey, we located the occulomotor complex by the distinctive unitary activity related to eye position. The well-modulated, eye-position-related firing rates make these cells readily identifiable. We then identified the magnocellular region of the red nucleus (RNm) as the group of cells that were located slightly lateral and caudal to the occulomotor complex and related to contralateral limb movements.

The area immediately above the RNm is relatively quiet. Upon entering the magnocellular division of the red nucleus, the change in activity is quite dramatic. The number of recorded units increases markedly, as does the amplitude of the individual action potentials. This generally heightened activity gives rise to a three- to fourfold increase in the average background activity, on which is imposed large action potentials of 500–2000 μV amplitude. During limb movement, RNm neuronal firing rate increases from 0–20 Hz spontaneous rate, to 200–400 Hz. The RNm has a well-documented somatotopy, which aids in its physiological identification. Virtually all forelimb-related units are located within the dorsomedial region of the nucleus, while the hindlimb cells are within the ventrolateral region.

During the last week of recording for each monkey, electrolytic lesions were placed at several recording sites. After all recordings were completed, the monkey was deeply anaesthetized with a lethal dose of sodium pentobarbitone and perfused with physiological saline followed by 10% neutral-buffered formalin. The brain was removed and blocked in the plane of the electrodes, and 40 μm thick frozen sections were cut in the frontal plane. The sections were mounted and stained with Luxol Fast Blue and Cresyl Violet. Electrode tracks, lesions and anatomical boundaries of the nucleus were identified and compared with the co-ordinates of each recorded cell. The few cells found to fall outside these anatomical boundaries were not considered for analysis.

The limb containing the EMG electrodes was dissected, and the location of each recording electrode was confirmed. We intended to implant both extensor digitorum communis (EDC) and extensor digitorum 4 and 5 (E4,5) in monkey BR, but the histological examination revealed that both electrodes had been implanted on EDC.

Data collection and analysis

These methods of data collection and analysis have been described in detail in an earlier publication (Houk, Dessem, Miller & Sybirska, 1987). The microelectrode signals were amplified and filtered, and action potentials from single neurons were discriminated with a level or window discriminator. The 1 ms discriminator output pulses were then low-pass filtered (10 ms time constant) to produce a signal proportional to the firing rate of the cell. EMG signals were amplified and full-wave rectified. These signals were also fed to 10 ms low-pass filters in order to avoid introducing phase shifts between the neuronal and EMG signals. The signals were sampled at 200 Hz, and stored on a magnetic disk for subsequent analysis. Data files of 1–2 min duration were collected while the monkey performed a single free-form task. For a given unit, we attempted to record at least one data file for each behavioural task. During these experiments, we also collected data during a visually guided tracking task. Those data will be the topic of a subsequent report.

A computer program allowed us to scan the raw data and set cursors to measure time intervals between particular events. In order to analyse mean firing rate during selected segments of the data files, we plotted cumulative spike count *versus* time. The depth of modulation for the activity in a particular file was determined by subtracting the spontaneous rate from the mean burst rate of the largest three to five bursts.

The principal time series analysis that we applied to the data was the cross-correlation equation. let $n(t)$ represent the discharge rate of an RNm neuron and let $m(t)$ represent the EMG recorded from a single muscle. The cross-correlation between n and m is given by:

$$R_{\mathrm{nm}}(\tau) = T \xrightarrow{\text{limit}} \infty \frac{1}{T} \int_0^T n(t)\, m(t+\tau)\, \mathrm{d}t, \tag{1}$$

where T is the duration of the data records, and $R_{nm}(\tau)$ is the average product of the two signals, as a function of the time shift τ introduced between the signals. Two signals which modulate in phase with each other will tend to have a large average product. The relation is analogous to the linear correlation coefficient if eqn (1) is normalized as follows:

$$\rho_{nm}(\tau) = \frac{R_{nm}(\tau) - \mu_n \mu_m}{\sigma_n \sigma_m}, \quad (2)$$

where μ and σ are the mean and variance of the signals respectively. This function yields values of ± 1 for perfect correlations and a value of 0 for no correlation. The cross-correlations were computed in the frequency domain, using the NEXUS signal analysis of software (Hunter & Kearney, 1984). The data were put into windows in 256-point segments, and linear trends were removed from each segment prior to the calculation.

Because the statistical significance of cross-correlations is not well defined, we used a Monte Carlo method to estimate the probability that correlation peaks of a given value would occur randomly. In order to preserve the spectrum of each signal while eliminating causal relations between signals, we transposed the first and second halves of the RNm rate signal. Using this transformed signal, we calculated the full set of cross-correlations and computed histograms showing the distribution of the randomly occurring peak values. We computed a total of 252 of these cross-correlations, and most had a peak with magnitude smaller than 0·10. There were fourteen (5·6%) correlations larger than 0·14 and eight (3·2%) larger than 0·15. Hence a reasonable estimate of the 5% level of significance is $\rho_{max} = \pm 0{\cdot}15$. Because there were so few correlations of magnitude larger than 0·15, it was impossible to make a reliable estimate of higher levels of significance.

In order to measure the extent to which particular muscles were activated in each task, we calculated average power of the EMG signals. We initially low-pass filtered the EMG signals (corner = 5 Hz) in order to remove high-frequency power related to the shape of motor unit action potentials, and then computed the sum of squared voltage for each sample point divided by the number of points in the signal.

As a test for cross-talk between muscles, we calculated the high-frequency coherence between muscle pairs. Cross-talk causes significant coherence at all frequencies, not only the low frequencies typical of physiological co-activation (Houk *et al.* 1987). We calculated the mean coherence squared in the frequency range 20–100 Hz for all combinations of muscles for two randomly chosen sets of fifteen files from monkeys AL and BR. Because of the very large number of combinations of muscles, it was impractical to make this calculation for all data files. Next we calculated the mean value for each muscle pair across the fifteen files. Finally, we calculated the mean and standard deviation for this set of values. Coherence squared greater than 2 standard deviations above the mean for any given pair was considered to be evidence of significant cross-talk.

RESULTS

We recorded RNm single unit and limb muscle activity while monkeys performed three food-retrieval tasks. The activity of hand and finger muscles necessary to form a precision grasp, scoop food from a well, or curl the fingers around a barrier differed substantially, yet individual RNm neurons were highly active during each of these tasks. Our goal was to understand how single RNm neurons contribute to the control of limb muscle activity, and more specifically, how they contribute to the control of reaching and grasping.

Movement-related EMG activity

Prehension task

The prehension task was the simplest and most stereotyped of the three free-form tasks. The monkey typically reached immediately toward the food as it was presented, grasped it, and returned it to his mouth to eat it. The reaching and grasping portions of this movement have been studied extensively by Jeannerod and

his colleagues (Jeannerod, 1984, 1988). He has divided the task into two functional components: 'transportation' and 'manipulation'. The transportation component involves the proximal muscles and joints which move the hand and arm toward the target, whereas the 'manipulation' component includes movements of the hand and fingers in anticipation of and during the grasp.

Figure 2 shows a set of EMG records spanning a 4 s segment of data taken from an 80 s long data file. The segment encompasses a single execution of the task and the EMG signals have been arranged from the most distal at the top to the most proximal near the bottom. Below the last EMG record are markers indicating the time of occurrence of several kinematic phases of the movement. Where possible, we have adopted terminology similar to that of Jeannerod. Time 0 is chosen to correspond to the onset of the muscle activity which extended the limb toward the target, here referred to as the 'transport phase'. The onset of transport was typically marked by bursts in triceps (Tri) and extensor (ECU) and flexor carpi ulnaris (FCU, not shown). Increased activity in extensor digitorum communis (EDC) at approximately this time was also typical. This abrupt increase of activity typically occurred among the different muscles within 100 ms. In some cases, the activity in triceps continued throughout the transport phase, along with that of biceps. However, depending on the initial location of upper arm and forearm, elbow extension could be accomplished largely by gravity. First dorsal interosseous (FDI, not shown) often had early activity within the transport phase, probably related to opening the hand and spreading the fingers.

Preceding the onset of transport, as the forearm was lifted from its resting position in front of the monkey, we have defined a 'preparation phase'. During this period, brachialis (Bra), anterior deltoid (ADl) and biceps (Bic) were active, and low-level activity in EDC and flexor digitorum sublimis (FDS, not shown) was also common. The onset of activity in EDC and FDS often preceded that of triceps by as much as several hundred milliseconds, although the timing was quite variable from trial to trial.

Several hundred milliseconds after the onset of the transport phase the intrinsic hand muscles became active, as the monkey grasped the food. Flexor pollicis brevis (FPB) and the 2nd lumbrical (Lum) are pictured as examples. We consider this the beginning of the 'grasp' phase. Activity in many other muscles was also typical during the grasp phase, although not necessarily well correlated with that of the intrinsic muscles. For example, the proximal muscles ADl and biceps continued to be active throughout the time the arm was extended.

Following grasp, we have defined a fourth component, the 'return' phase, which is marked by an abrupt reduction in intrinsic muscle activity and in activity of ADl. The decreased ADl activity allowed backward movement of the humerus to occur passively, and it was often accompanied by a burst of activity in brachialis, which assisted in flexing the elbow. There was typically relatively little other muscle activity in this phase. Brachialis was rarely active in this task for periods longer than 500 ms, and typically fired in short bursts. It was inactive in this task more frequently than any other muscle. Greater activity during other tasks (e.g. single joint elbow movements) convinced us that the muscle activity had been recorded properly. The marked difference between biceps and brachialis activity is probably

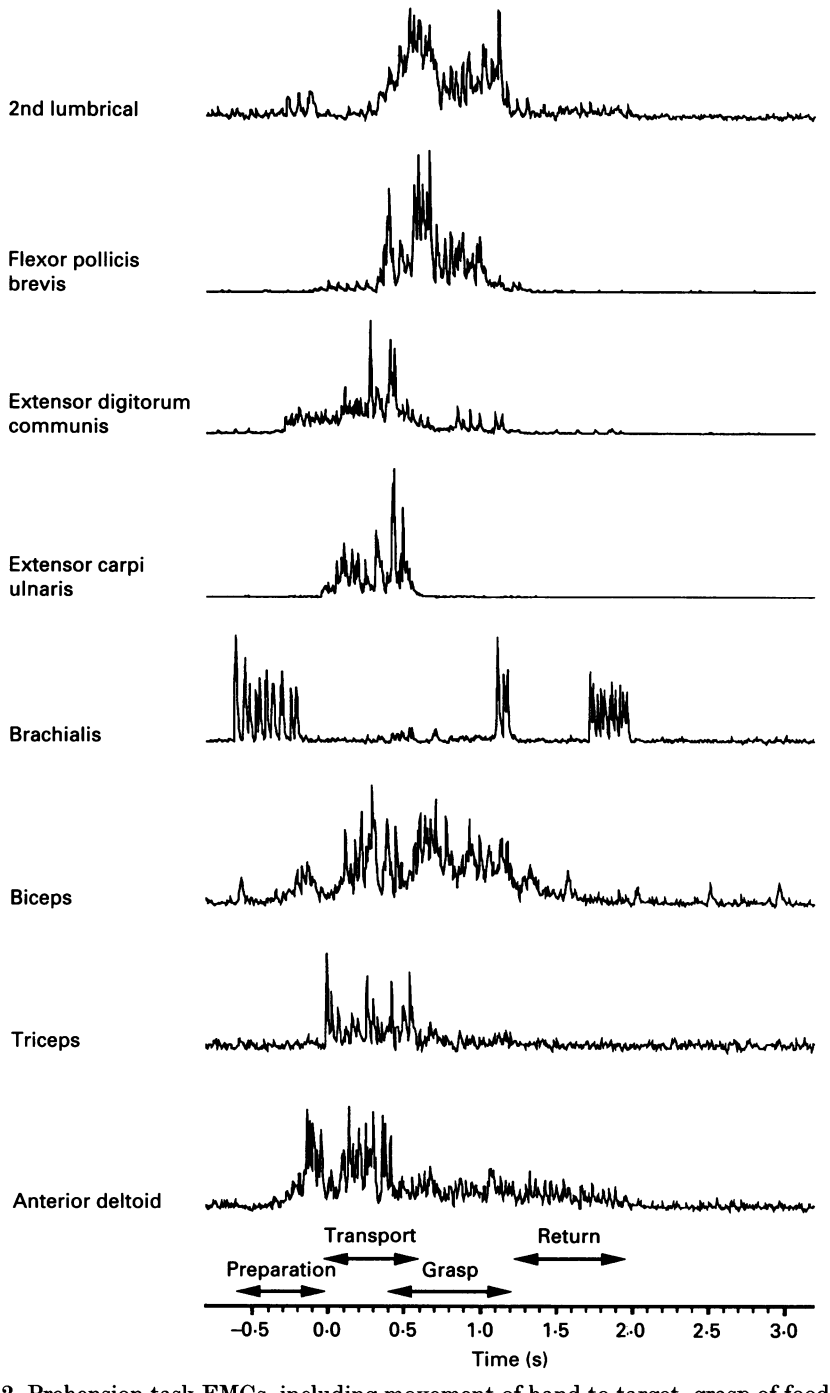

Fig. 2. Prehension task EMGs, including movement of hand to target, grasp of food, and return of hand to mouth. General increase of activity occurs around time 0 as arm begins to move toward target (transport phase). Intrinsic hand muscle activity peaks during grasp phase, at which time wrist and common digit muscles relatively quiet.

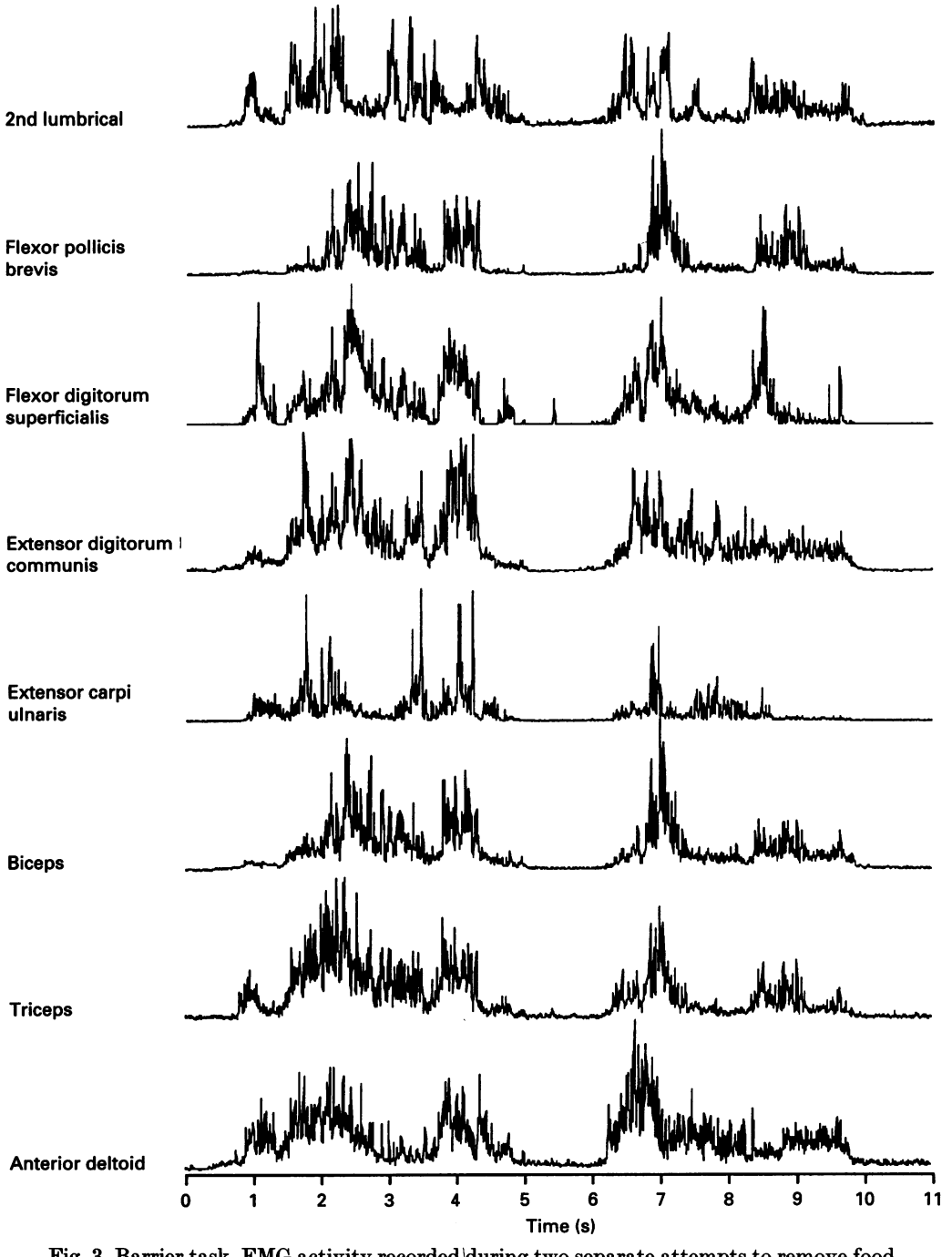

Fig. 3. Barrier task. EMG activity recorded during two separate attempts to remove food from a ledge shielded by a clear plastic barrier. The onset of activation for both periods was more nearly synchronous than was typical of the prehension task and there was considerable co-activation of many muscles throughout both periods. As a result, during

the result of the different geometry of the two muscles. Biceps crosses both elbow and shoulder; its maintained activity was necessary to provide appropriate shoulder torque. Brachialis is a pure elbow flexor, which accounts for its inactivity during arm extension.

Although the four phases of the task were generally recognizable, there was considerable variation in timing from trial to trial. Most prominent was variation in the duration of a particular phase or in the latency between phases. Additional muscle names abbreviated in later figures, but not referred to here include: flexor carpi radialis (FCR), flexor digitorum profundus (FDP), flexor pollicis brevis (FPB), and adductor pollicis (AdP).

Barrier task

While the prehension task was highly stereotypic, the 'barrier' task required highly varied movements from trial to trial. The monkey was required to retrieve food from behind a transparent barrier held by the experimenter. The food was placed on a small ledge on the back side of the barrier and in order to grasp the food the monkey was forced to reach around the small barrier. The position in space and the orientation of the barrier were varied from trial to trial, forcing the monkey to adopt changing strategies. More time was typically required for each successful trial, as the monkey often made a number of abortive attempts before successfully grasping the food.

Figure 3 shows two of these prolonged attempts to grasp the food, separated by a brief pause. As anticipated, the temporal patterns of the EMG were more varied for different reaches during the barrier task than during the prehension task. As a result, there was no 'typical' temporal sequence. The onset of a given trial could generally be recognized by the nearly synchronous onset of activity in many muscles of the limb. We rarely saw the distinct phases which were typical of prehension. In particular, there was rarely any early, anticipatory activity in either EDC or FDS as the hand approached the barrier. We did not anticipate the amount of co-activation that was typically present during this task. Most muscles had a more varied and complex temporal pattern than during the prehension task, but typically many of the muscles recorded at the same time had patterns that were quite similar to one another. This resulted in greater phasic activity in the proximal muscles than was typical of the prehension task, which was presumably necessary to stabilize the distal limb during the rapid searching movements around the barrier. These points are well illustrated by the two major periods of activity in this figure. Within either period, the activation of most of the muscles resembled one another quite closely, yet the patterns during the two periods of activity differed substantially.

Kluver task

The third free-form task required the monkey to remove small pieces of food from the holes of a Kluver board (Kluver, 1957). The kinematics and patterns of muscle

---

either period of activity, a large number of muscles had very similar patterns. For most muscles the pattern during the second period of activity differed substantially from that of the first period, presumably the result of a different behavioural strategy.

activation during this task differed substantially from that of either the prehension task or the barrier task. Whereas the barrier task tended to emphasize proximal muscle activation, the Kluver board task had somewhat greater distal muscle involvement. Figure 4 shows a segment of EMG data recorded while monkey AL performed this task. The emphasis on distal muscle activity is apparent from the bursts of activity of the intrinsic hand muscles as well as FDS and ECU. The bursts coincided with the finger movements to retrieve a raisin from a well. During the series of bursts beginning at approximately 3·5 s, the triceps was tonically active in order to hold the arm extended toward the board. After seven attempts to grasp the raisin, triceps activity abruptly decreased, and bursts occurred in biceps and ADl, which returned the hand to the mouth. In many cases brachialis (not shown) was also phasically active at this time. This number of bursts was larger than usual; the monkey typically retrieved the food with fewer attempts. A similar sequence, including only two finger movements, occurred at the beginning of this record. In summary, the Kluver task was characterized by rhythmic bursts of distal muscle activity which occurred during finger movements, and alternated with activity in the proximal muscles to extend and withdraw the arm.

Average EMG power

In order to determine the extent to which the various muscles were used in the three free-form tasks, we calculated the average power in each of the EMG signals during each task. This analysis was made only for the data recorded from monkey AL. For most muscles, the maximum power occurred during the barrier task, except for brachialis and FPB, which had greater power during the Kluver task. All muscles were active in each task, with the occasional exception of biceps, which often was only weakly activated during the Kluver task.

Analysis of cross-talk between muscles

The level of cross-talk between muscles was analysed by computing the high-frequency coherence between pairs of muscles. For monkey BR, the mean coherence squared between all seventy-eight pairs of muscles was $0{\cdot}067 \pm 0{\cdot}032$. A single pair had mean coherence squared of 0·30. Histological analysis revealed that these electrodes, which were intended for muscles EDC and E4,5 had actually been implanted on two different sites on EDC. Data from only one of the pair was used for further analysis. No other muscle pairs exceeded 2 standard deviations above the mean, although three pairs, FDS–FCU (0·13), AdP–FDI (0·13) and Lum–FDI (0·12) were just under this value. For monkey AL, the mean coherence squared between all pairs of muscles was $0{\cdot}050 \pm 0{\cdot}013$. Despite the generally lower values of coherence for this monkey, the smaller standard deviation resulted in two muscle pairs (among 66 combinations) having values exceeding 2 standard deviations above the mean. These were ECU–EDC (0·11) and AdP–Lum (0·10).

These results indicate that there was some tendency for agonist muscles in close proximity to one another to have high-frequency coherence somewhat above mean levels. However, given the relatively small size of the effect, and the fact that these particular muscle pairs were strongly co-activated in these tasks, the amount of cross-talk is likely to be quite low.

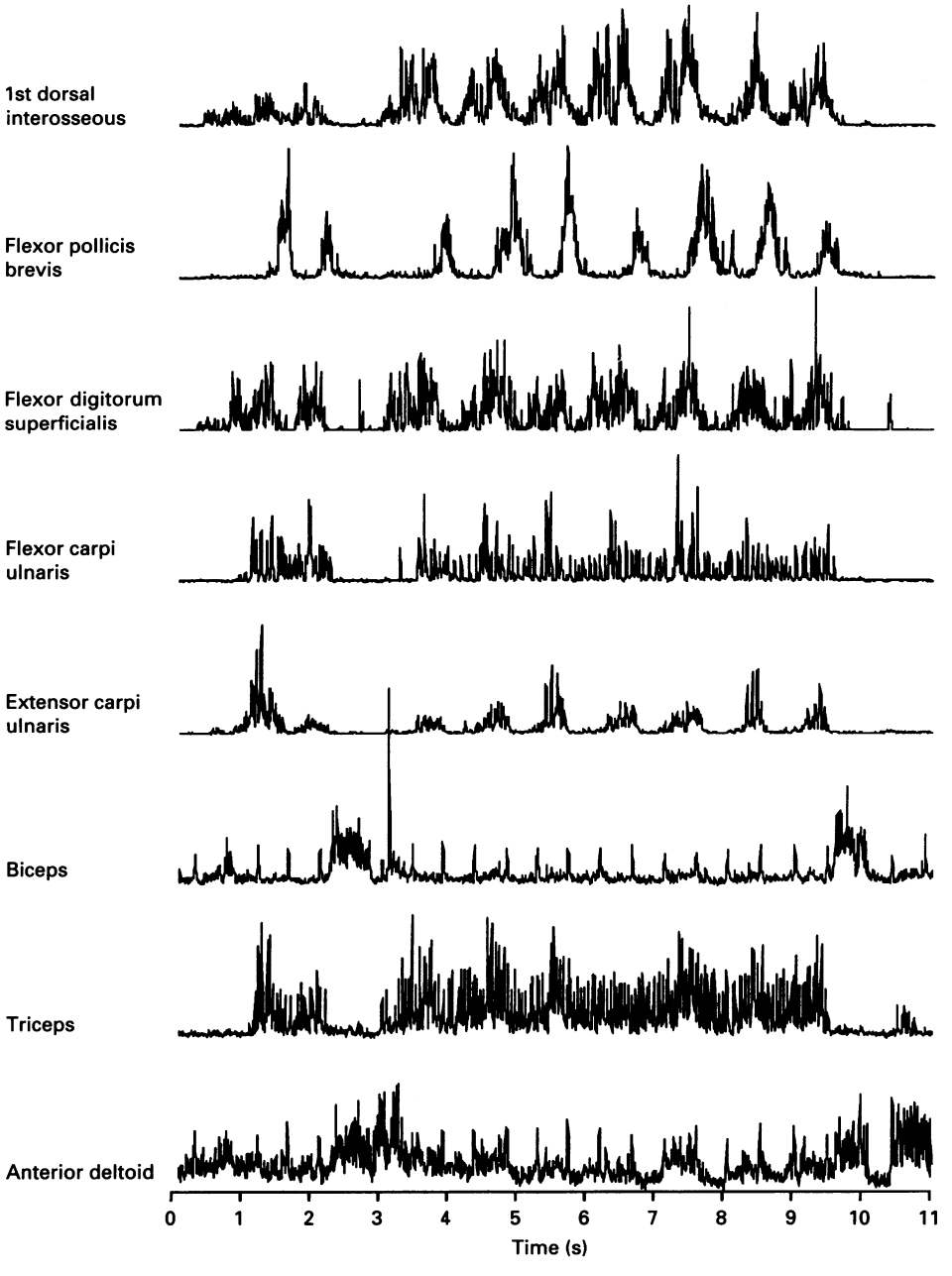

Fig. 4. Kluver task. Distal EMGs reflect rhythmic finger movements to retrieve food from wells. Triceps was tonically active to keep limb extended toward board. Biceps was active phasically at 2 and 9 s to return the hand to mouth. Artifacts caused by the electrocardiogram are evident in biceps and anterior deltoid signals.

Movement-related RNm activity

We isolated and recorded from eighty-four identified RNm forelimb neurons of monkey BR, seventy-four from monkey AL, sixty-one from monkey GU, and twenty from monkey MQ. Most of these units discharged vigorously in association

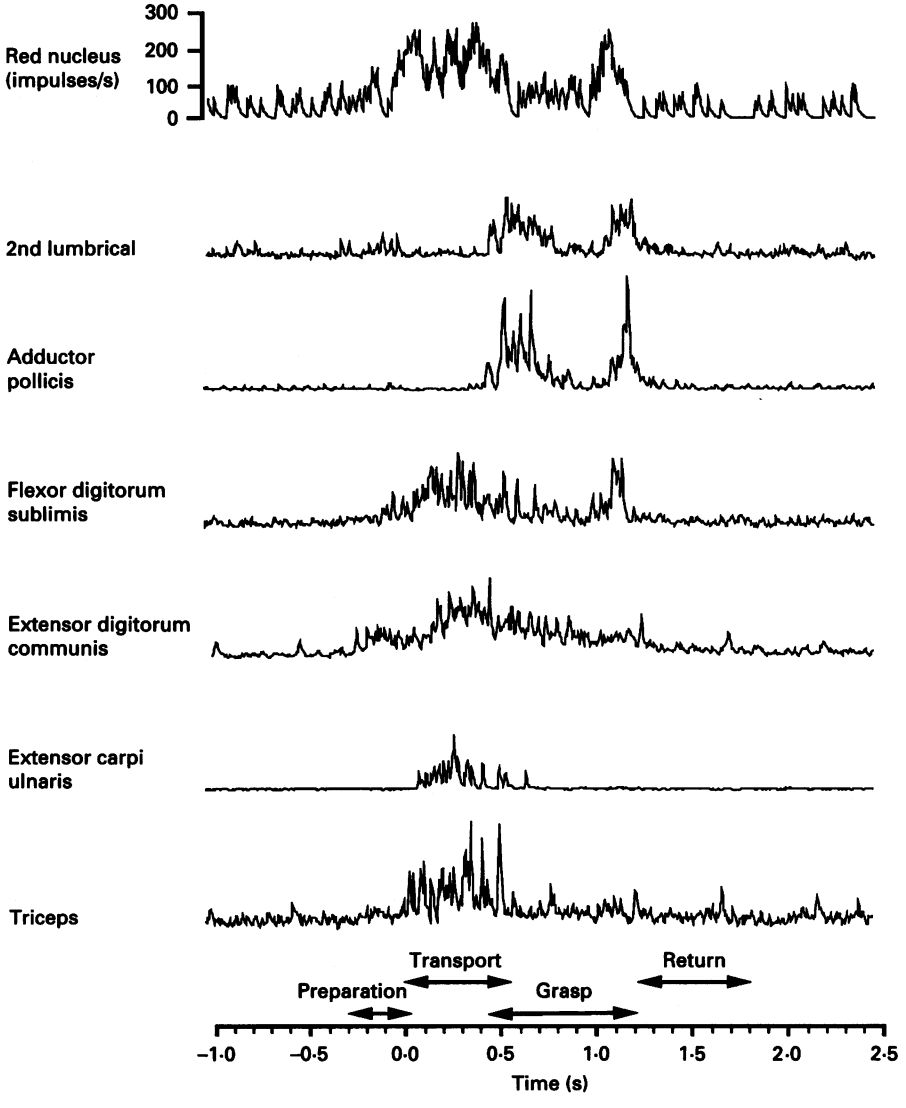

Fig. 5. RNm and EMG activity during prehension (AL187). The neuron (top trace) was most active during the transport phase of movement. The initial burst preceded the activity of FDS and EDC and declined shortly before the onset of intrinsic muscle activity.

with performance of the free-form movement tasks. Figure 5 shows a segment of data including EMG activity and RNm neuron discharge during a single execution of the prehension task. The neuronal activity consisted of several discrete bursts which

reached a peak rate of nearly 300 impulses/s, and had a mean rate of 190 impulses/s. RNm discharge during the free-form tasks typically consisted of several 250–500 ms duration bursts separated by short pauses. Most units fired at a low and variable rate (0–20 impulses/s) during the periods between movements. Often this background firing increased slightly several hundred milliseconds before movement onset. We chose a set of thirty-nine strongly task-related neurons from monkeys AL and GU based on the strength of the cross-correlations between RNm and EMG activity. We calculated the depth of modulation for all the data files from these neurons. For individual neurons, we often found large differences in the neuronal discharge during the different tasks. The depth of modulation for the best-related free-form task was typically 125–150 impulses/s. However, across all neurons, the mean discharge did not differ significantly for the different tasks (t test; 5% significance).

During a recording session, it was often obvious that certain units were primarily active during the early proximal limb movement, whereas others were active during the later finger movements. We undertook a more detailed classification of the burst timing by examining the activity of twenty strongly task-related neurons from each of the monkeys AL, BR, and GU. For each neuron, we determined the times of occurrence of the different phases of the prehension task and of the accompanying bursts of neuronal activity. Seventy per cent of the well-related units had significant activity in the transport phase, and 60% were active during grasp. Only 15% of the units had significant activity in the preparation or return phases. These numbers total more than 100% since neurons frequently were active in more than one phase.

Cross-correlations between RNm and EMG

The difficulty of relating neural discharge to arbitrary behavioural parameters or features of the EMG can be appreciated in Fig. 5. The major burst of activity for this particular neuron was restricted largely to the transport phase and bore most resemblance to the activity of FDS. The activity dropped significantly for nearly 500 ms within the grasp phase during the period of greatest intrinsic activity but increased in a second, shorter burst of activity near the end of the phase. This late burst was accompanied by activity in FDS as well as several of the intrinsic hand muscles. Often the timing or reliability of the relation varied during repeated movements. In this example, intrinsic hand muscle activity in one case was accompanied by a burst of RNm activity, while earlier EMG activity in the same muscles occurred in the absence of neuronal activity

The cross-correlation function provides an objective method of comparing these patterns. The peak correlation (ρ_{max}) indicates the similarity of the two signals; the time of the peak indicates the relative timing between the two signals. Figure 6 shows cross-correlations between discharge of the transport-phase neuron and each of the EMGs shown in Fig. 5. The cross-correlations were calculated from the full 85 s data file recorded during the prehension task, from which the records in Fig. 5 are only a short segment. Each cross-correlation summarizes the relation between the neuron and a particular muscle. The full set of cross-correlations reveals how this neuron was related to the different muscles that were active during the task.

Figure 5 suggests that FDS activity was closely related to that of the neuron, and the cross-correlations support this observation. The peak value of $\rho_{max} = 0{\cdot}42$ occurred at lag $\tau = 30$ ms. The positive lag indicates that the EMG activity followed

that of the neuron. EDC was nearly as well correlated as FDS, although this is not as obvious from Fig. 5. Neither AdP nor Lum was significantly correlated with the unit (i.e. $\rho_{max} \geqslant 0{\cdot}15$), despite the single RNm burst (at about 1 s in Fig. 5) which coincided with a brief period of their activity.

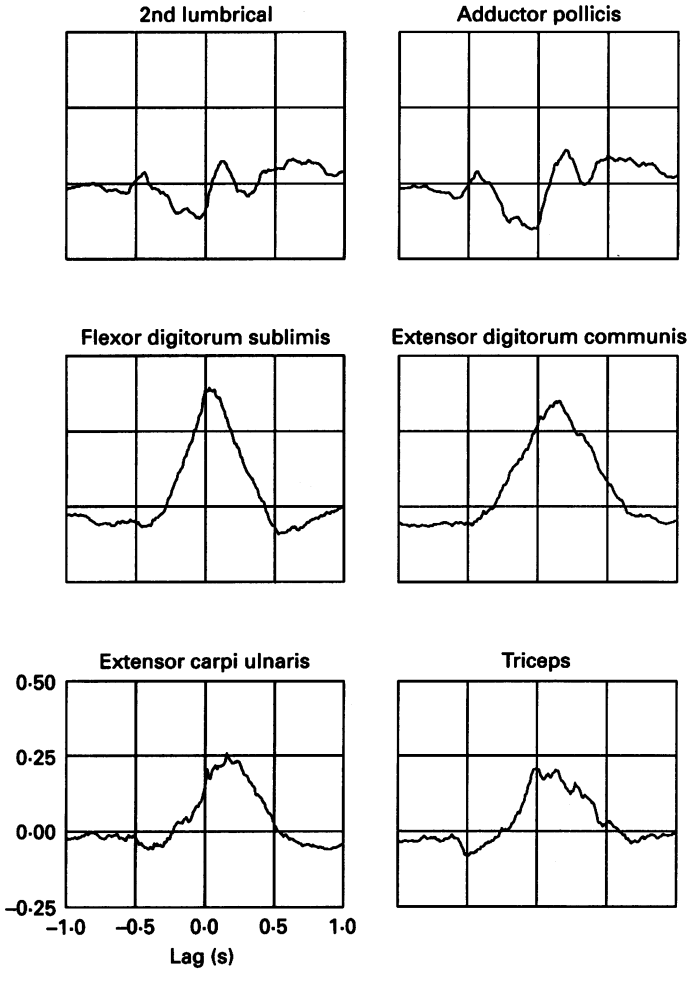

Fig. 6. RNm–EMG cross-correlations for the transport-phase neuron during the prehension task (Fig. 5). The entire file was 85 s long. FDS and EDC had the largest peaks, which occurred at short positive lag (RNm leading EMG). Intrinsic muscles were uncorrelated, as were other, unshown muscles.

The neuronal activity depicted in Fig. 5 was predominant during the transport phase of the prehension task. Activity during the grasp phase of prehension was also typical of many RNm neurons. Figure 7 shows an analysis of a grasp-phase neuron, which resulted in strong cross-correlations with Lum, AdP, and FPB. The largest of these had a peak value of $\rho_{max} = 0{\cdot}43$. In marked contrast to the cross-correlations for the transport-phase neuron shown in Fig. 6, the cross-correlations with EDC and FDS were below the 5% level of statistical significance. The only additional muscle

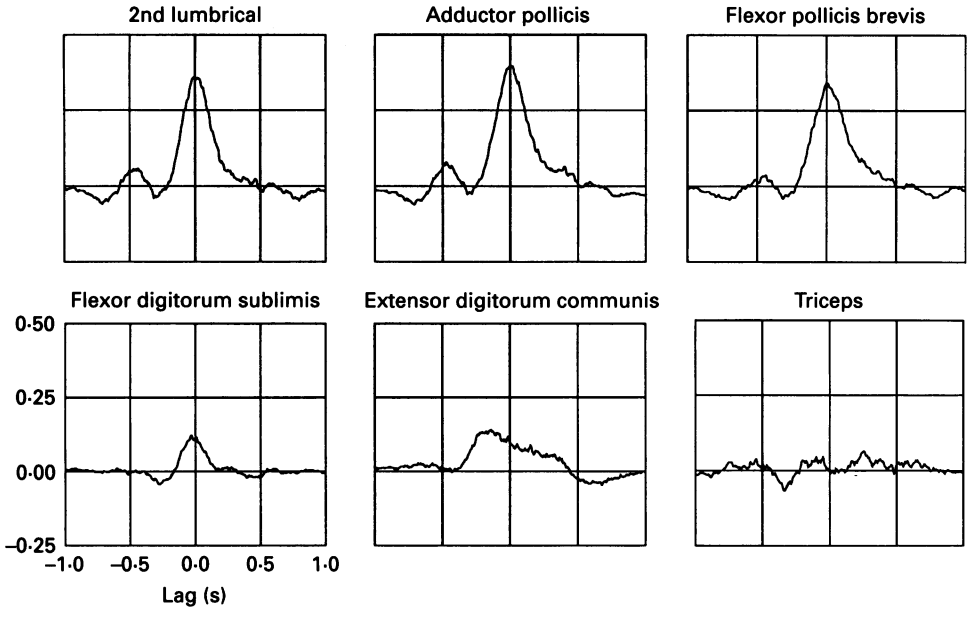

Fig. 7. Cross-correlations for a grasp-phase neuron during the prehension task. Three intrinsic muscles were strongly correlated; EDC and FDS were not.

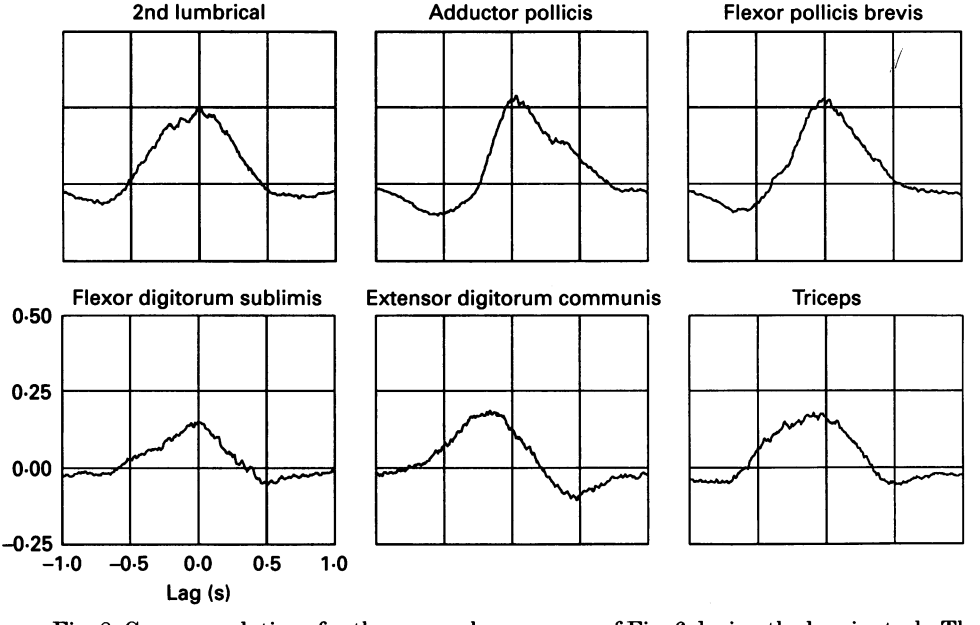

Fig. 8. Cross-correlations for the grasp-phase neuron of Fig. 6 during the barrier task. The same three intrinsic muscles were best correlated, but several other muscles were also weakly correlated.

with a significant correlation was FDI, another intrinsic hand muscle. Figure 8 shows cross-correlations for this neuron during the barrier task. As during the prehension task, Lum, AdP, and FPB were the three best-correlated muscles. However, there

was less difference between the height of these peaks and those of the more weakly related muscles. This was primarily the result of decreased correlation among the intrinsic muscles, as well as slightly increased correlations among other muscles.

Magnitude and timing of the peak correlations

Figures 6 and 7 include several of the largest correlations we measured. These figures also show that some muscles remained uncorrelated even though the neuron

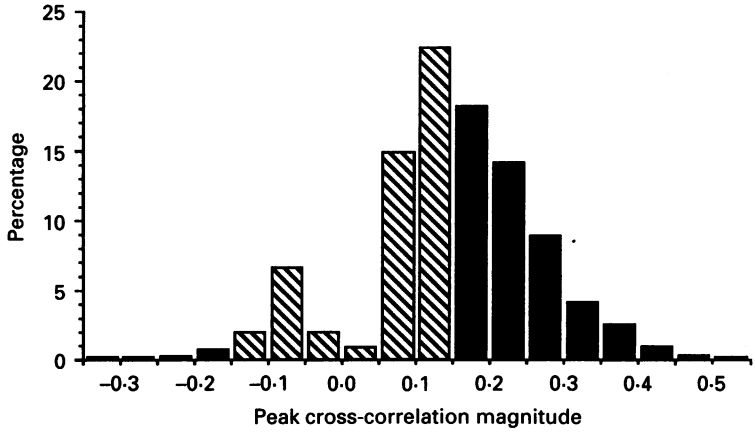

Fig. 9. Distribution of cross-correlation magnitude for 3904 RNm–EMG pairs from all monkeys. Nearly all statistically significant correlations were positive. Correlations near 0 almost never occurred because even unrelated signals virtually always had chance correlations with magnitude above 0·05. ■, Statistically significant ($P < 0·05$); ▨, not significant.

was strongly task related. Figure 9 is a histogram showing the distribution of these RNm–EMG peak cross-correlation values for 3904 pairs of neurons and muscles. The distributions for the four monkeys were virtually indistinguishable, so the data have been combined. Although the distribution was bi-modal, ρ_{max} was approximately 5–7 times more likely to be positive than negative. This observation underscores the observation, made frequently before, that RNm discharge tends to increase rather than decrease during limb movement, during the period when muscle activity is increasing as well. The small number of negative correlations represent muscles which have major activity in phases other than that of the maximal RNm activity.

For monkeys AL and BR, we collected data during each of the three free-form tasks. The correlations obtained during the prehension task were significantly higher than those of the Kluver and barrier tasks (t test; $P < 0·01$). The rank order of the three tasks was prehension, Kluver and barrier. The mean correlation for each of these tasks was 0·18, 0·15 and 0·12 respectively, for monkey AL, and 0·16, 0·12 and 0·11 for monkey BR. Data collection was less systematic for monkey GU, but the results were similar.

The time of the peak cross-correlation indicates the time lag between two signals. The timing is meaningful, of course, only if the two signals are strongly correlated.

When considering timing, we adopted a highly conservative criterion, well above the 5% level of statistical significance, by considering only those cases having $\rho_{max} \geqslant 0{\cdot}25$. Figure 10 shows the distribution of these lags for monkeys AL and BR, including the 528 of 3136 (17%) neuron–muscle pairs that were correlated above this

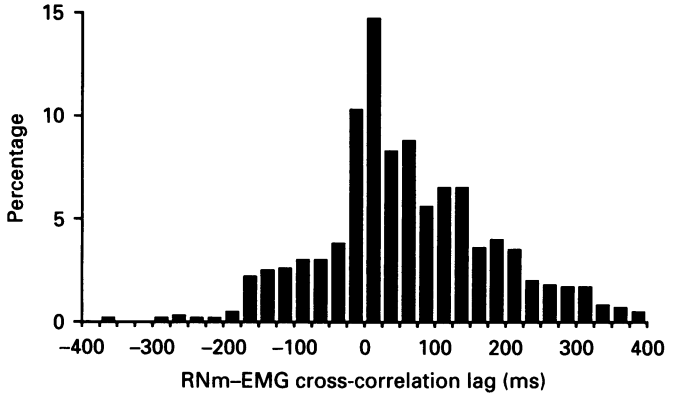

Fig. 10. Timing of the peak RNm–EMG cross-correlation for 528 neuron–muscle pairs from monkeys AL and BR which had $\rho_{max} \geqslant 0{\cdot}25$. Positive lag occurred when EMG activity followed that of the RNm.

level. Approximately 85% of the peaks fell between −150 and 200 ms. The distribution had a single modal value near 25 ms, and mean of 52 ms. When weaker (but statistically significant) correlations were added to this distribution, the range of lags became much greater.

Functional linkage vectors

The set of cross-correlations provides a simple, quantitative means of summarizing the relation between the patterns of activity of the neuron and the patterns of activity of the n muscles that were monitored. For each data file, we defined a 'functional linkage vector' as the set of n ρ_{max} values for the n RNm/EMG cross-correlation functions. The functional linkage vector points in a direction in n-dimensional muscle space that identifies those muscles that are best correlated with the unit. The term 'functional' has been chosen because the cross-correlation determines the strength of an arbitrary dynamic, linear function between the single unit signals and EMG. This term should be distinguished from the similar, 'synaptic linkage vector', each element of which is the strength of the post-spike facilitation (or suppression) for a particular muscle, determined by spike-triggered averaging (Miller *et al.* 1992).

Table 1 summarizes these data for the twenty neurons most strongly related to EMG activity during the prehension task. Each row of the table expresses a single functional linkage vector from monkey AL or BR. Blank entries correspond to muscles of a given monkey that were not recorded. Those entries greater than or equal to 0·25 are indicated with an asterisk. When more than one prehension task data file was recorded from a given neuron, only the single best correlated case was

considered. Generally a given neuron was closely related to more than one muscle. At each joint (excluding the intrinsic hand muscles which have more complex actions) extensor muscles were more strongly and more frequently correlated with neuronal activity than were flexors. There was also a tendency for distal muscles to be better correlated than proximal muscles. These observations are particularly clear if one

TABLE 1. Strongest functional linkage vectors for monkeys AL and BR

File	Bic	Bra	Tri	FCU	ECR	ECU	FDP	FDS	EDC	FPB	AdP	Lum	FDI
BR592	—	0·16	0·09	0·12	0·25*	0·35*	0·26*	0·29*	0·56*	0·19	0·34*	0·46*	0·32*
BR182	—	−0·13	0·26*	0·10	0·21	0·53*	0·36*	0·39*	0·37*	0·21	0·38*	0·24	0·37*
BR696	—	0·15	0·14	0·12	0·19	0·48*	0·38*	0·32*	0·53*	0·40*	0·36*	0·41*	0·41*
AL145	0·11	−0·10	0·28*	0·20	—	0·34*	—	0·41*	0·51*	0·37*	0·31*	0·24	0·40*
AL123	0·20	0·06	0·39*	0·14	—	0·26*	—	0·43*	0·38*	0·35*	0·48*	0·40*	0·45*
BR443	—	0·21	0·13	0·22	0·21	0·26*	0·18	0·23	0·47*	0·28*	0·26*	0·37	0·27*
BR272	—	0·24	0·09	0·28*	0·16	0·12	0·13	0·33*	0·14	0·16	0·19	0·44*	0·26*
BR756	—	0·37*	0·19	0·22	0·23	0·28*	0·36*	0·20	0·36*	0·26*	0·41*	0·43*	0·43*
AL156	0·10	0·07	0·07	0·05	—	0·15	—	0·13	0·16	0·37*	0·43*	0·39*	0·19
BR734	—	0·14	0·24	0·15	0·15	0·37*	0·22	0·31*	0·25*	0·35*	0·36*	0·42*	0·38*
AL087	0·08	0·07	0·35*	0·36*	—	0·28*	—	0·42*	0·39*	0·39*	0·27*	0·12	0·42*
AL187	0·08	−0·06	0·23	0·17	—	0·28*	—	0·42*	0·39*	0·13	−0·15	−0·11	0·21
BR577	—	0·21	0·10	0·11	0·17	0·17	0·12	0·17	0·41*	0·11	0·21	0·21	0·19
AL107	0·25*	0·20	0·24	0·22	—	0·27*	—	0·38*	0·36*	0·32*	0·41*	0·29*	0·40*
BR217	—	0·18	0·20	0·17	0·10	0·36*	0·16	0·28*	0·35*	0·25*	0·39*	0·32*	0·38*
BR243	—	0·20	0·26*	0·17	0·22	0·20	0·23	0·30*	0·39*	0·36*	0·32*	0·28*	0·36*
BR547	—	0·27*	0·08	0·18	0·36*	0·33*	0·23	0·30*	0·30*	0·38*	0·39*	0·30*	0·37*
AL019	0·25*	0·33*	0·20	0·21	—	0·28*	—	0·39*	0·20	0·28*	0·17	0·29*	0·26*
BR288	—	−0·13	0·36*	0·09	0·23	0·34*	0·26*	0·35*	0·35*	0·34*	0·38*	0·17	0·38*
BR415	—	0·15	0·23	0·08	0·24	0·31*	0·24	0·30*	0·37*	0·28*	0·29*	0·23	0·28*
Best	0	0	0	0	0	1	0	3	7	0	6	3	3

Functional linkage vectors for the 20 best correlated neurons from monkeys AL and BR during prehension. Those muscles with $\rho_{max} \geqslant 0{\cdot}25$ are marked with an asterisk. Bottom row lists number of times each muscle was best correlated, emphasizing a distal, extensor muscle bias.

considers only the single best-correlated muscle for each neuron. Indicated in the bottom row of the table is the number of times each muscle was the most highly correlated of the set. EDC and AdP were most prominent among these highly correlated muscles. There was only a single case in which a muscle proximal to the hand was best correlated (BR182, ECU).

There was considerable variety in the functional linkage vectors for different neurons. For example, unit BR272 was much better related to wrist and digit flexion than it was to extension. Unit AL156 was unrelated to the common digit flexors and extensors, whereas its correlations with most of the intrinsic hand muscles were quite strong. In contrast, unit AL187 had its strongest correlations with the common digit muscles. BR577 was exclusively related to EDC.

Functional linkages within tasks

In order to compare any two linkage vectors, we constructed a scatter plot between the individual elements of the two vectors. The correlation coefficient of the resulting cluster of points indicates how nearly the two vectors resemble each other. If the vectors were nearly identical, the points would fall along a straight line and

yield a large correlation coefficient. If there were no similarity between the vectors, the correlation would be near zero. A systematic difference between the vectors such that those muscles which were strongly correlated for one file were weakly correlated for the other, would result in a negative correlation. This analysis had the advantage that it did not require that individual correlations be judged as either 'significant' or 'insignificant'. However, linkage vectors composed entirely of elements near the limit of statistical significance would be expected to vary randomly, and add noise to the analysis. Therefore, linkage vectors were used only if at least one element had magnitude greater than 0·20.

Figure 11 demonstrates the use of scatter plots to compare the linkage vectors calculated for several different neurons during the prehension task. Included are the transport-phase neuron of Figs 5 and 6 (AL187), the grasp-phase neuron of Fig. 7 (AL156), and a third neuron used as a control (AL123). Figure 11*B* shows the linkage vector for the transport-phase neuron plotted against that of the grasp-phase neuron. Both neurons were related primarily to distal muscles of the limb but differed in the specific muscles that were best related. In one case the extrinsic hand muscles were strongly correlated, in the other the intrinsics. This is reflected by the negative slope of the regression line. In order to test the reliability of the linkage vectors, we divided data files into two equal length segments, and calculated a full set of cross-correlations for each half. The scatter plot shown in Fig. 11*C* demonstrates the high similarity of the resulting vectors for this example. For a small number of neurons we made the same comparison between two data files collected during the prehension task from a given neuron. In many cases, collection of these two files was separated by 10–15 min, since we typically tested the other two free-form behaviours, as well as a visually guided tracking task using five different manipulanda, before repeating the prehension task.

Only monkeys AL and BR had a sufficiently large number of reliably recorded muscles to perform this analysis. For monkey AL, there were 378 comparisons among 27 different neurons, and 13 divided-file cases. The filled bars in panel *D* represent the comparisons between same-unit linkage vectors, and the hatched bars are the comparisons of different units. There was a 15-fold higher probability of obtaining a correlation above 0·8 for the same-unit comparisons than for different-unit comparisons, and there were more small and negative correlations for the different-unit comparisons. The mean of the different-unit distribution (0·33), was significantly less than that of the same-unit distribution (0·66; unpaired t test, $t = 3{\cdot}7, P < 0{\cdot}001$). A single comparison for a neuron which was recorded twice during the prehension task yielded a correlation of 0·74. For monkey BR, there were eight cases in which a single unit was tested twice during the prehension task. The mean of these 8 comparisons was 0·69. In addition, there were 400 comparisons between forty-one different neurons for monkey BR. The distribution of r values for different-unit linkage vectors had a mean of 0·37, which was also significantly smaller than the same-unit comparisons ($t = 3{\cdot}3; P < 0{\cdot}001$). In summary, during the prehension task, there was much greater similarity between two linkage vectors for a given neuron than between the linkage vectors of different neurons.

Functional linkages across tasks

We also tested the extent to which the linkage vectors were dependent on the monkey's behaviour by comparing the linkage vectors for a given neuron during each of the three behavioural tasks. For monkey AL, comparisons were made for fifteen

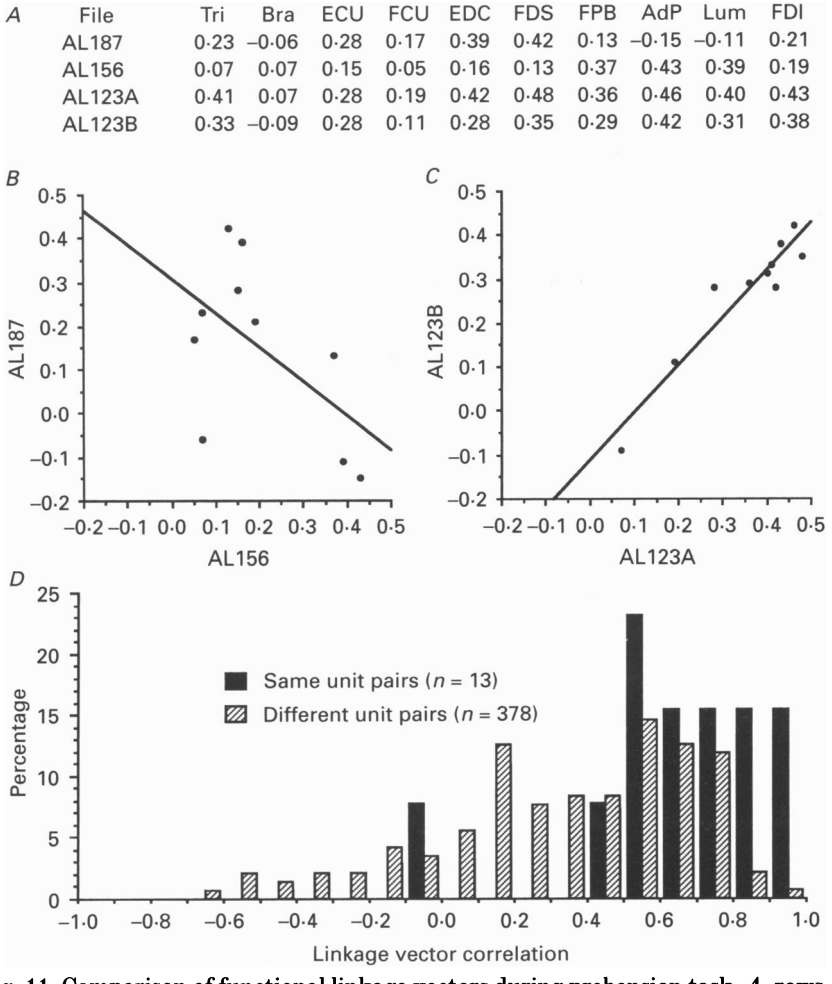

Fig. 11. Comparison of functional linkage vectors during prehension task. *A*, rows contain linkage vectors for a transport neuron (Figs 5 and 6, AL187), grasp neuron (Fig. 7, AL156) and first and second halves of a file from a third neuron which was active in both phases (AL123A and AL123B). *B*, negative correlation between the elements of the transport and grasp neurons resulted because the two neurons had very different functional roles during the prehension task. *C*, strong positive correlation resulted from the comparison of linkage vectors for two halves of a single file. *D*, hatched bars show distribution of correlation coefficients for 144 pairs of linkage vectors from different neurons during prehension (monkey AL). The many negative and small positive correlations indicate the variety of linkage vectors for different neurons. Filled bars indicate the much greater similarity of control cases like that of panel *C*.

neurons that were well related to both the prehension and barrier tasks, and eight neurons that were well related to the prehension and Kluver tasks. This yielded 23 same-unit comparisons, and 744 same-task comparisons. For monkey BR there were 19 prehension–Kluver pairs and 12 prehension–barrier pairs, yielding 31 same-unit and 955 same-task comparisons.

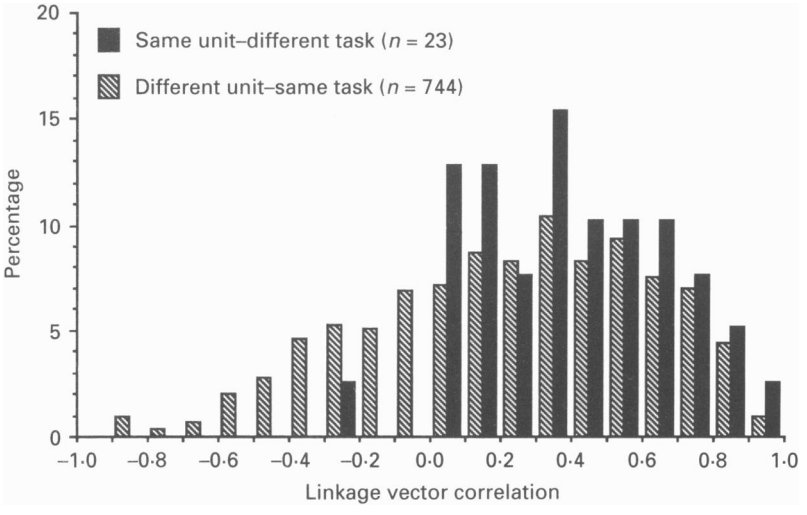

Fig. 12. Comparison of linkage vectors for different tasks. Linkage vectors for a particular neuron varied during different tasks (filled bars), but there was much more variation between different neurons during a single task (hatched bars).

Figure 12 shows the distribution of comparisons for monkey AL. The filled bars represent the comparisons of the same neuron during different tasks and the hatched bars are for different neurons during the same task. There was a greater similarity resulting from the same-unit comparisons (mean value = 0·39) than for the same-task comparisons (mean value = 0·23). The mean values of the two populations were significantly different ($t = 2{\cdot}5$; $P < 0{\cdot}01$). The similarity of the same-cell comparisons was considerably less than that of the control comparisons (same-cell and same-task) shown in Fig. 11*D*. This indicates that the linkage vectors depended to some extent on behaviour. The same analysis for monkey BR yielded results which were consistent with those of monkey AL, except that the mean of the same-cell condition (0·28) was substantially lower, and therefore not significantly different from the mean of the same-task condition (0·23).

DISCUSSION

Muscle activity during reaching and grasping

The ability to make stable, long-term EMG measurements from a large set of hand and arm muscles allowed us to study these free-form movements rather than to be constrained to simpler, one- or two-dimensional movements, the kinematics of which

can be more easily measured. The prehension task we used is similar to that studied in human subjects by Jeannerod and colleagues. They have described adjustments in the size of the grip as the hand approaches the target which depend on the size and shape of the object (Jeannerod, 1988). There is considerable overlap in time between grip adjustments and the movements of the limb toward the target (Jeannerod, 1984). These two components of the movement are closely coupled kinematically when the location of the object is unexpectedly perturbed (Paulignan, Mackenzie, Marteniuk & Jeannerod, 1989).

During prehension in our experiments, the common digit muscles EDC and FDS, as well as the intrinsic hand muscle FDI, were often activated prior to activation of triceps. The activity in EDC and FDS probably corresponds to the anticipatory adjustments of grip size and shape described by Jeannerod. The action of FDI is to abduct the index finger. This may correspond to a general spreading of the digits as the hand was opened. Despite its similarity to the prehension task during the initial phases of movement, this early activity was typically absent during the barrier task. Such activity would have been of little use in shaping the hand, given the unpredictability of the required hand posture during the period when the limb was moving toward the barrier. This observation highlights the context-dependent nature of the coupling between the proximal and distal limb.

Significance of RNm discharge during movement

A traditional means of studying the motor system in behaving animals has been to look for neurons with activity patterns closely resembling some feature of a single, learned behaviour. Although often very compelling, these observations alone cannot be considered final evidence of a causal relation between the particular neuronal activity and behaviour. Necessary supporting evidence includes the demonstration of anatomical connections and the effects of lesions. The majority of rubrospinal neurons terminate within interneurons ultimately projecting to motoneurons serving muscles of the limbs (Sprague, 1948; Sterling & Kuypers, 1967). Terminals have also been demonstrated among motoneurons of the distal limb (McCurdy, Hansma, Houk & Gibson, 1987; Holstege, 1987). Spike-triggered averaging has been used to infer the presence of synaptic connections between individual RNm neurons and particular muscles (Mewes & Cheney, 1991; Miller *et al.* 1992). Lesions of the RNm or rubrospinal tract interfere particularly with co-ordinated hand use in the monkey (Lawrence & Kuypers, 1968) and the cat's ability to grasp food with its paws (Sybirska & Gorska, 1980; Alstermark, Lundberg, Norrsell & Sybirska, 1981).

Having established the underlying anatomical substrate necessary for a neuron to control these movements, two problems remain. First one must judge whether the activity of a particular neuron is task related and behaviourally 'significant'. Many different definitions of significance have been applied to this question. Second, among those neurons having significant task-related activity, it is important to determine how the activity is related to the task, both spatially and dynamically. The presence of invariant relations in the spatial or temporal coding between the neuronal activity and particular aspects of the behaviour provides additional information about the nature of the control system.

Generally, the degree of task relation has been judged by comparison of firing rates before and after movement onset. One approach has been to apply statistical tests

to the recorded spike intervals to select statistically significant changes. This apparently reasonable approach has the disadvantage that quite small changes in discharge rate may become statistically significant for neurons with fairly uniform spontaneous firing rates, particularly when the statistics are calculated across data segments of several seconds duration. In order to identify a population of task-related motor cortical cells, Thach (1978) was compelled to select only those cells having burst rates which differed from background with significance of $P < 0{\cdot}00001$. Criteria based on a minimum change in mean firing rate have also been used. Gibson, Houk & Kohlerman (1985*a*) restricted their analysis to neurons having modulation greater than 50 impulses/s during movement.

The free-form tasks described in this paper were well suited to the study of the RNm, because of the very large percentage of neurons which were strongly activated during the movements. Depth of modulation of 50–100 impulses/s was typical in our experiments, 100–200 was not uncommon. Other tasks, for example, single joint tracking, may also produce large bursts of activity, but in a much smaller number of cells (Gibson, Houk & Kohlerman, 1985*a*; Cheney, Mewes & Fetz, 1988). There can be little question, even by the most conservative measures, that this activity was task related, and 'significant'. However, a brisk neuronal burst during the movement may not necessarily be well correlated with a particular phase of the movement, or the activity of particular limb muscles. The cross-correlation function provided a means of determining the strength of the relations.

Two factors which are typically considered to indicate a strong relation between neuronal activity and EMG (or movement) are the relative timing of the two signals, and the dynamical relation between the amplitudes of the signals. The cross-correlation function combines these two criteria, as both consistent timing and linear dynamics are required for a large magnitude cross-correlation. Because there was essentially no subjective judgement required on the part of the experimenter, the method was both objective and efficient.

Strength of the cross-correlation between neuron and muscle activity

Each point τ of the cross-correlation between sampled signals x and y is equivalent to a linear correlation coefficient calculated between pairs of points x_i and $y_{i+\tau}$. $(\rho_{max})^2$ is analogous to the coefficient of determination, the output variance which is accounted for by the best static, linear model of the input. The best $(\rho_{max})^2$ values for the top twenty neurons of Table 1 ranged from 0·12 to 0·31. For a small number of cases, we also calculated the variance accounted for by a linear dynamic model, and this yielded broadly similar results. How then, are we to interpret the significance of neuronal activity which is linearly related to only 10–25 % of the activity of the best related muscle? From anatomical considerations alone, the contribution of any single neuron in the RNm must be virtually negligible against that of the entire population of RNm and motor cortical neurons. Hence if one makes the (unreasonable) assumption that the activity of these neurons was uncorrelated with other neurons projecting to the same muscles, one would expect to find much less variance accounted for. The fact that we have found correlations of this magnitude emphasizes that the signals from many other (unrecorded) neurons may be well correlated with that of the individually recorded neurons.

There have been very few other attempts to calculate long time-span cross-

correlations (including lags in the order of seconds) between central neurons and EMG activity. Spike-triggered averaging studies have been more numerous, using spikes recorded from neurons in a variety of central structures. Although the two methods are very closely related, spike-triggered averaging has been focused almost exclusively on the events at very short time lags around individual spike events. Typically the effect of neighbouring (both preceding and following) spikes has been treated as noise. In contrast, we have been most interested in the long time-span effects, which are dependent chiefly on bursts of spikes, rather than individual spikes.

We have previously reported similar results for data obtained from cats (Houk *et al.* 1987). Another study was that of Soechting, Burton & Onoda (1978), who calculated point process cross-correlations between a small number of RNm neurons and biceps muscle EMG in cats trained to make repetitive elbow flexion movements. Although they showed several such correlations, they did not report their magnitude, so it is impossible to make a direct comparison with our results. Quantitative measures of correlation between premotor neuronal activity and movement or EMG have been calculated by several other techniques. Lamarre and colleagues calculated mean values of motor cortical neuron firing rate, biceps and triceps EMG, and velocity and acceleration while monkey subjects made alternating elbow movements (Lamarre, Spidalieri & Lund, 1981). They constructed scatter plots between mean neuronal discharge rate and EMG for repeated trials. The linear correlation coefficients for the two reported examples were 0·40 and 0·45. The same analysis between discharge rate and velocity and acceleration yielded somewhat higher correlations (Lamarre, Spidalieri, Busby & Lund, 1980; Lamarre *et al.* 1981).

The same technique was used more extensively by Gibson *et al.* (1985*b*), in order to compare RNm discharge and movement dynamics. They identified a small set of neurons which had large correlations between neuronal activity and movement parameters. Within this group, correlations between mean spike rate and movement velocity ranged from approximately 0·5 to greater than 0·9. They did not measure EMG in conjunction with the neuronal measurements.

A hybrid technique was used to examine cerebellar cortical and deep nuclear cells during movements of a joy-stick in response to a visual target (Marple-Horvat & Stein, 1987). Ensemble averages of discharge rate and movement were first calculated, and then cross-correlations were calculated between the averages. Peak correlations between discharge rate and velocity were within the range of 0·4 to 0·95. Concurrent EMG measurements were not made.

The large correlations found in the Gibson *et al.* (1985*b*) and the Marple-Horvat & Stein (1987) studies are probably due to several sources. Most important is the time or ensemble averaging prior to calculation of the correlation, which reduces the random, uncorrelated variation in both signals. In addition, both averaging techniques considered only a short segment of data surrounding, or restricted to, a single stereotyped movement and excluded the poorly correlated neuronal activity between movements. Furthermore, any trial-to-trial variation in timing between discharge and movement would reduce the magnitude of the cross-correlation without affecting the time-averaged, static correlations.

The fact that we measured EMG rather than movement signals is another possible explanation for the small magnitude of our cross-correlations, but it is difficult to

evaluate this because of the other potentially larger differences caused by the variety of analytical methods. Unfortunately, we were unable to monitor the free-form movement trajectories, so we cannot make this direct comparison.

Co-ordinate system of the activity

Each element of the n-dimensional functional linkage vector expresses the similarity between the neuronal activity and that of a particular limb muscle. The larger the element, the more nearly alike were the two signals. Taken as a whole, the vector can be thought of as expressing the direction in muscle space of the neuronal signal. A neuron which was correlated only with EDC, for example, would have direction parallel to the EDC axis. On the other hand, a neuron with activity like that of both EDC and ECU would fall between these two axes, more nearly parallel to the axis of the muscle with which it bore the greatest resemblance.

A two-dimensional space may be divided into 2^2 or 4 quadrants. By analogy, the 10-dimensional muscle space may be divided into 2^{10} or 1024 'quadrants'. The functional linkage vector representing an RNm unit having all positive correlations (even if they were insignificantly small), would fall within the first, or positive quadrant. This would include the majority of the correlations between RNm units and EMG. Thus these vectors are restricted to approximately 0·1 % of the entire space. However, the vectors do not completely fill even this restricted region, since large positive correlations with the proximal limb flexor muscles, for example, were relatively infrequent. On the other hand, correlations with the wrist and digit extensors occurred quite frequently. This suggests that the vectors tended to form clusters within the first quadrant.

Visualizing these clusters within a high dimensional space is not a trivial problem. However, it is easy to calculate angles between pairs of vectors as a measure of their similarity. The cosine of the angle is simply the dot product of two vectors. Vectors confined to a single quadrant would yield no angles larger than 90 deg. In this respect, calculation of the correlation coefficient, which is closely related to the cosine, has certain advantages. The correlation coefficient is obtained by first computing the mean values of the elements for each of the two vectors. The mean for each vector is then subtracted from each of its elements, and the cosine is calculated between the resulting vectors. Subtracting the (positive) mean causes those elements of the vector which were near zero to become negative, so that the resulting vector is no longer restricted to the positive quadrant of the muscle space. This makes it possible to find large negative correlation coefficients, which are analogous to angles approaching 180 deg, between vectors which are actually restricted to a single quadrant. Two similar vectors will be shifted approximately equally, and the angle between them will remain small. This proved to be a more sensitive measure of linkage vector similarity than did calculation of the cosine.

The correlation coefficient between linkage vectors for different neurons was frequently near zero or negative. These cases demonstrate the great variety of linkage vectors throughout the population of neurons. There were also numerous cases in which the linkage vectors of different neurons were very similar. This should come as no great surprise, as one would expect many RNm neurons to share similar discharge properties. The linkage vectors for a particular cell and different tasks were

more nearly alike than were those for different cells and a single task. However, there was not a great difference between the means of two groups. To some extent, the variation in linkage vectors must be due to the stochastic nature of the signals. However, this source is unlikely to explain all of the variation. Some feature of the behaviour, for example, its predictability, may cause the RNm to play a different role in the movement. It is possible that the connections between RNm neurons and motoneurons are modulated, at least functionally, by the altered behaviour. Perhaps RNm discharge encodes some other aspect of the behaviour, such as muscle force or hand movement, more reliably than it does muscle activation.

In addition to the correlations mediated by connections between RNm neurons and motoneurons, some correlations will also result from connections between, and common input to, premotoneurons. This could hypothetically include motor cortical as well as RNm neurons. These connections presumably serve to co-ordinate the activity of the many premotoneurons controlling the movement, and may be fundamental to the production of the movement command (Houk *et al.* 1993). Any neuron having activity which closely reflects the aggregate activity of a population of neurons will be correlated with those muscles controlled by the population, regardless of whether it has connections to those muscles. To the extent that these premotor interconnections are dependent on behaviour, the indirect correlations will be as well. The use of spike-triggered averaging in combination with long time-span cross-correlation may be valuable in distinguishing between these sources of correlation. Simultaneous recordings from several premotoneurons may also be necessary to evaluate the importance of the interactions at that level.

The work of Georgopoulos and colleagues (Georgopoulos *et al.* 1982, 1984) has provided an important demonstration of a fundamental spatial property of the discharge of motor cortical cells. Individual motor cortical neurons are tuned such that they are activated maximally during movements made in a particular 'preferred' direction. The discharge in other directions is proportional to the cosine of the angle between the movement direction and the cell's preferred direction.

An analogy can be made between our analysis using a muscle co-ordinate system and the analysis employed by Georgopoulos and his colleagues. A cell with a preferred direction along an axis pointing away from the monkey (y-axis) has, by definition, its greatest discharge for movements along this axis. Correlations between the discharge and the y-component of movements along the y-axis would be large, whereas correlations for movements along the x-axis would be very small. Because of the cosine tuning of these cells, movements made 45 deg to the right of the preferred direction would be accompanied by a discharge approximately 70% of that in the preferred direction; the amplitude of the y-component of the movement would also be reduced to approximately 70%. Since both the discharge and the y-component of movement are simply scaled, the y-axis cross-correlation would remain approximately the same as it was for movements in the preferred direction. Since for a 45 deg movement, the x- and y-components of the movement are equal, the x- and y-axis correlations would be identical. Movements 45 deg to the *left* of the preferred direction would produce the same magnitude correlations as those to the *right*, but the x-axis correlation would be negative. For a series of movements made in all directions, only the correlation with the y-component of movement (the preferred

direction) would be reliable; that with the x-component would approach zero. Similar arguments can be advanced for cells with any preferred direction. The magnitude of the correlation with any particular axis would be proportional to the movement-related discharge along that axis. Therefore, the linkage vector obtained in world co-ordinates should point approximately in the preferred direction.

While the spatial tuning of a motor cortical cell is evident in a world co-ordinate system, it does not necessarily imply that the cells encode those spatial features of the movements directly. Mussa-Ivaldi has shown that a muscle-based co-ordinate system may also be used to describe these results (Mussa-Ivaldi, 1988). It may be that at the highest levels of the nervous system, some neurons do directly encode spatial features of limb movements. Clearly at the lowest level, mononeurons carry signals which are encoded in an intrinsic co-ordinate system determined by the geometry of the musculo-skeletal system. It would be of great interest to record both movement and EMG signals along with RNm or motor cortical activity. Functional linkage vectors could be calculated for muscle and world co-ordinate systems, and tested during different types of behaviour. Such information should make it possible to determine whether the discharge of central neurons codes the activation patterns of muscles, or parameters of movement.

REFERENCES

ALLEN, G. I. & TSUKAHARA, N. (1974). Cerebrocerebellar communication systems. *Physiological Reviews* **54**, 957–1006.

ALSTERMARK, B., LUNDBERG, A., NORRSELL, U. & SYBIRSKA, E. (1981). Integration in descending motor pathways controlling the forelimb in the cat. 9. Differential behavioral defects after spinal cord lesions interrupting defined pathways from higher centres to motoneurones. *Experimental Brain Research* **42**, 299–318.

BERTHIER, N. E., SINGH, S. P., BARTO, A. G. & HOUK, J. C. (1991). Distributed representation of limb motor programs in arrays of adjustable pattern generators. *Technical Report 3: Center for the Study of Neuronal Populations and Behavior.*

CHENEY, P. D., MEWES, K. & FETZ, E. E. (1988). Encoding of motor parameters by corticomotoneuronal (CM) and rubromotoneuronal (RM) cells producing postspike facilitation of forelimb muscles in the behaving monkey. *Behavioral Brain Research* **28**, 181–191.

FORTIER, P. A., KALASKA, J. F. & SMITH, A. M. (1989). Cerebellar neuronal activity related to whole-arm reaching movements in the monkey. *Journal of Neurophysiology* **62**, 198–211.

GEORGOPOULOS, A. P., KALASKA, J. F., CAMINITI, R. & MASSEY, J. T. (1982). On the relations between the direction of two-dimensional arm movements and cell discharge in primate motor cortex. *Journal of Neuroscience* **2**, 1527–1537.

GEORGOPOULOS, A. P., KALASKA, J. F., CRUTCHER, M. D., CAMINITI, R. & MASSEY, J. T. (1984). The representation of movement direction in the motor cortex: Single cell and population studies. In *Dynamic Aspects of Neocortical Function*, ed. EDELMAN, M., GAIL, W. E. & COWEN, W. M., pp. 501–524. Wiley, New York.

GIBSON, A. R., HOUK, J. C. & KOHLERMAN, N. J. (1985*a*). Magnocellular red nucleus activity during different types of limb movement in the macaque monkey. *Journal of Physiology* **358**, 527–549.

GIBSON, A. R., HOUK, J. C. & KOHLERMAN, N. J. (1985*b*). Relation between red nucleus discharge and movement parameters in trained macaque monkeys. *Journal of Physiology* **358**, 551–570.

HOLSTEGE, G. (1987). Anatomical evidence for an ipsilateral rubrospinal pathway and for direct rubrospinal projections to motoneurons in the cat. *Neuroscience Letters* **74**, 269–274.

HOUK, J. C. (1989). Cooperative control of limb movements by the motor cortex, brainstem and cerebellum. In *Models of Brain Function*, ed. COTTERILL, R. M. J., pp. 309–325. Cambridge University Press, Cambridge.

HOUK, J. C., DESSEM, D. A., MILLER, L. E. & SYBIRSKA, E. H. (1987). Correlation and spectral analysis of relations between single unit discharge and muscle activities. *Journal of Neuroscience Methods* **21**, 201–224.

HOUK, J. C., KEIFER, J. & BARTO, A. G. (1993). Distributed motor commands in the limb premotor network. *Trends in Neurosciences* **16**, 27–33.

HUNTER, I. W. & KEARNEY, R. E. (1984). Nexus: A computer language for physiological systems and signal analysis. *Computers in Biology and Medicine* **14**, 385–401.

JEANNEROD, M. (1984). The timing of natural prehension movements. *Journal of Motor Behavior* **16**, 235–254.

JEANNEROD, M. (1988). *The Neural and Behavioral Organization of Goal-Directed Movements*. Clarendon Press, Oxford.

KALASKA, J. F., COHEN, D. A. D., PRUD'HOMME, M. & HYDE, M. L. (1990). Parietal area 5 neuronal activity encodes movement kinematics, not movement dynamics. *Experimental Brain Research* **80**, 351–364.

KLUVER, H. (1957). *Behavior Mechanisms in Monkeys*. Chicago University Press, Chicago.

KUYPERS, H. G. J. M. (1981). Anatomy of the descending pathways. In *Handbook of Physiology*, section I, *The Nervous System*, vol. II, part 1, ed. BROOKHART, J. M., MOUNTCASTLE, V. B., BROOKS, V. B. & GEIGER, S. M., pp. 597–666. American Physiological Society, Bethesda, MD, USA.

LAMARRE, Y., SPIDALIERI, G., BUSBY, L. & LUND, J. P. (1980). Programming of initiation and execution of ballistic arm movements in the monkey. In *Progress in Brain Research*, vol. 54, *Motivation, Motor and Sensory Processes of the Brain*, ed. KORNHUBER, H. H. & DEECKE, L., pp. 157–169. Elsevier, Amsterdam.

LAMARRE, Y., SPIDALIERI, G. & LUND, J. P. (1981). Patterns of muscular and motor cortical activity during a simple arm movement in the monkey. *Canadian Journal of Physiology and Pharmacology* **59**, 748–756.

LAWRENCE, D. G. & KUYPERS, H. G. J. M. (1968). The functional organization of the motor system in the monkey. II. The effects of lesions of the descending brain-stem pathways. *Brain* **91**, 15–36.

LOEB, G. E. & GANS, C. (1986). *Electromyography for Experimentalists*. The University of Chicago Press, Chicago.

MARPLE-HORVAT, D. E. & STEIN, J. F. (1987). Cerebellar neuronal activity related to arm movements in trained rhesus monkeys. *Journal of Physiology* **394**, 351–366.

MCCURDY, M. L., HANSMA, D. I., HOUK, J. C. & GIBSON, A. R. (1987). Selective projections from the cat red nucleus to digit motor neurons. *Journal of Comparative Neurology* **265**, 367–379.

MEWES, K. & CHENEY, P. D. (1991). Facilitation and suppression of wrist and digit muscles from single rubromotoneuronal cells in the awake monkey. *Journal of Neurophysiology* **66**, 1965–1977.

MILLER, L. E., HARRIS, G. D. & HOUK, J. C. (1989). Chronic EMG implants used to study the relations between red nucleus discharge and limb muscle activity during a variety of tasks. *Society for Neuroscience Abstracts* **15**, 172.

MILLER, L. E., SINKJAER, T., ANDERSEN, T., LAPORTE, D. J. & HOUK, J. C. (1992). Correlation analysis of relations between red nucleus discharge and limb muscle activity during reaching movements in space. In *Experimental Brain Research*, vol. 22: *Control of Arm Movement in Space: Neurophysiological and Computational Approaches*, ed. CAMINITI, R., JOHNSON, P. B. & BURNOD, Y., pp. 263–283, Springer-Verlag, Berlin.

MUSSA-IVALDI, F. A. (1988). Do neurons in the motor cortex encode movement direction? An alternative hypothesis. *Neuroscience Letters* **91**, 106–111.

PAILLARD, J. (1991). *Brain and Space*. Oxford University Press, New York.

PAULIGNAN, Y., MACKENZIE, C. L., MARTENIUK, R. G. & JEANNEROD, M. (1989). The coupling of arm and finger movements during prehension: Perturbation of object location. *Society for Neuroscience Abstracts* **15**, 49.

SINKJAER, T., ANDERSEN, T., MILLER, L. E. & HOUK, J. C. (1990). Cross correlation and spike triggered averages (STA) between monkey red nucleus and forelimb muscle electromyogram (EMG). *European Journal of Neuroscience*, suppl. 3, 66.

SOECHTING, J. F., BURTON, J. E. & ONODA, N. (1978). Relationships between sensory input, motor output and unit activity in interpositus and red nuclei during intentional movement. *Brain Research* **152**, 65–79.

SPRAGUE, J. M. (1948). A study of motor cell localization in the spinal cord of the Rhesus monkey. *American Journal of Anatomy* **82**, 1–28.

STERLING, P. & KUYPERS, H. G. J. M. (1967). Anatomical organization of the brachial spinal cord of the cat. II The motoneuron plexus. *Brain Research* **4**, 16–32.

SYBIRSKA, E. & GORSKA, T. (1980). Effects of red nucleus lesions on forelimb movements in the cat. *Acta Neurobiologiae Experimentalis* **40**, 821–841.

THACH, W. T. (1978). Correlation of neural discharge with pattern and force of muscular activity, joint position, and direction of next movement in motor cortex and cerebellum. *Journal of Neurophysiology* **41**, 654–676.